Soils and Foundations 2013;53(5):746–755

The Japanese Geotechnical Society

Soils and Foundations

www.sciencedirect.com
journal homepage: www.elsevier.com/locate/sandf

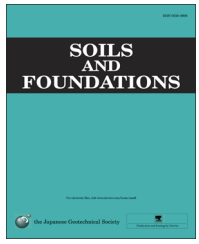

The inter-particle coefficient of friction at the contacts of Leighton Buzzard sand quartz minerals

Kostas Senetakis*, Matthew R. Coop, M. Cristina Todisco

Department of Civil and Architectural Engineering, City University of Hong Kong, Kowloon Tong, Kowloon, Hong Kong

Received 7 November 2012; received in revised form 27 June 2013; accepted 24 July 2013
Available online 26 September 2013

Abstract

A series of micro-mechanical tests was carried out in order to investigate the inter-particle coefficient of friction at the contacts of quartz minerals of Leighton Buzzard sand. For this purpose, a custom-built inter-particle loading apparatus was designed and constructed, the main features of which are described briefly in this paper. This apparatus is capable of performing shearing tests at the contacts of soil minerals of a particle–particle type in the range of very small displacements, from less than 1 μm to about 300 μm, and very small normal loads, between about less than 1 N and 15 N. The laboratory data showed that the effects of the normal force and the sliding velocity on the coefficient of dynamic friction are not significant, while dry and saturated surfaces had similar frictional characteristics. The steady state sliding was mobilized within a range of 0.5–3.0 μm of horizontal displacement, and the coefficient of static friction was very similar to the corresponding coefficient during constant shearing. Repeating the inter-particle shearing tests on the same particles and following the same shearing track indicated a small reduction in the inter-particle coefficient of friction after the first shearing, which is possibly related to plastic deformation and damage to the asperities.

1. Introduction

The complexity of the behavior of granular soils has been partially related to their particulate nature, the processes of particle breakage, the complex interaction mechanisms that dominate the response at the particle contacts and the morphology of the particles (e.g., McDowell and Bolton, 1998; Yimsiri and Soga, 2000; Soga and O'Sullivan, 2010; Cavarretta et al., 2010; Jo et al., 2011). Recent advances in the Discrete Element Method (DEM), proposed by Cundall and Strack (1979), have led to a more realistic simulation of the response of granular assemblies and a better understanding of the complex mechanisms that dominate the response of soils. In this direction, modern laboratory methods, such as the X-Ray CT technique, have been developed to quantify the response of particles within the soil mass. The methods give insight into the micro-mechanisms that dominate particulate media (e.g., Watanabe et al., 2012; Fonseca et al., 2012).

Using DEM, Yimsiri and Soga (2000) showed that when the response at the contacts of discrete particles is modeled taking surface roughness into account, the results from the numerical simulations are then closer to the real behavior observed in laboratory tests. In their DEM study, Wang and Yan (2012) showed that the contribution of particle breakage to the dissipation of energy is very small, but that the process of particle breakage promotes changes in the soil fabric. These

*Corresponding author.
E-mail address: ksenetak@cityu.edu.hk (K. Senetakis).
Peer review under responsibility of The Japanese Geotechnical Society.

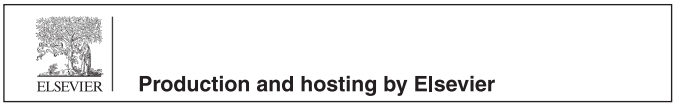

0038-0806
http://dx.doi.org/10.1016/j.sandf.2013.08.012

changes create an important energy dissipation mechanism, which is related to the frictional response at the contacts of the particles. It seems, therefore, that the laboratory findings by Consoli et al. (2007) and Senetakis et al. (2012, 2013a, 2013b), whereby the granular soils of variable mineralogies and particle morphologies show substantial differences in their static and dynamic properties, is possibly the result of the different energy dissipation mechanisms and the interactions of particles at their contacts even at very small shear strains.

Consequently, a better understanding of the behavior of soils, when treated as a continuum, necessitates a better understanding and a thorough study of the response of soil particles at their contacts. Recent DEM studies, that quantitatively examined the effect of the inter-particle coefficient of friction on the monotonic and cyclic responses of granular assemblies, have also supported this necessity. For example, Barreto and O' Sullivan (2012) showed that an increase in the inter-particle coefficient of friction, μ, increases the peak angle of the shearing resistance and the shear stiffness, and also that the dilative response is more pronounced. In their DEM study, Barreto and O'Sullivan also showed that parameter μ strongly affects the inherent stability of the strong force chains. In an earlier study by Thornton (2000), it was revealed that the increase in μ significantly affects the behavior of soils in the range of large strains by increasing the critical void ratio. The important role of the inter-particle coefficient of friction on the cyclic response of granular assemblies was also demonstrated by Sazzad and Suzuki (2011). They showed that the increase in μ decreases the width of the hysteretic loops, and that during unloading and when the inter-particle coefficient of friction is high, for example, higher than 0.8, parameter μ also affects the evolution of the coordination number.

Despite the increasing use of DEM and the perception that the micro-mechanical characteristics of soil particle contacts strongly affect the overall macro-scale response of granular assemblies, the laboratory work investigating the micro-mechanical characteristics of soils is still limited. Most experimental efforts have been focused on the normal load–deflection response and the compression strength of soil particles (e.g., Nakata et al., 1999; McDowell and Amon, 2000; McDowell, 2002; Cole and Peters, 2007, 2008; Cavarretta et al., 2010). Experimental works that include a study on the frictional characteristics of soils, particularly for the case when one particle is sheared on the surface of a second one, are extremely limited (e.g., Skinner, 1969; Procter and Barton, 1974; Cole et al., 2010; Cavarretta et al., 2010; Cavarretta et al., 2011). Instead, most studies presented in literature have been focused on sphere–flat or flat–flat types of contacts for both soil minerals (e.g., Horn and Deere, 1962; Cole et al., 2010) and artificial materials (e.g., Burwell and Rabinowicz, 1953; Baumberger et al., 1999; Baumberger and Carolim 2006; Berthoud et al., 1999; Krick et al., 2012), which can be implemented more easily in the laboratory.

Horn and Deere (1962) showed that while the frictional characteristics at the contacts of the minerals of a massive structure, such as quartz, are not significantly affected by the conditions of the test, i.e., dry or saturated surfaces, they noticed that the friction is much lower during steady state sliding when the surfaces are dry. Recently, Cole et al. (2010) showed that the response at the contacts of the minerals is highly hysteretic for both the range of very small deformations and during steady state sliding. The study by Cole et al. was focused, primarily, on experiments on the sphere–flat type of contacts with additional data for the sphere–sphere type on the artificially created surfaces of mixed mineralogy, while the work by Horn and Deere was focused on the flat–flat type of contacts of surfaces of single mineralogy. Cavarretta et al. (2010) presented inter-particle shearing tests on quartz minerals of a particle-particle type, which is more applicable for real soils, but their work was limited to the dynamic coefficient of friction during steady state sliding without any information on the range of very small deformations.

In this paper the frictional characteristics at the contacts of quartz minerals of a single type and of a particle–particle type are presented in both the range of very small deformations before the onset of steady state sliding and during constant shearing. Quartz particles of Leighton Buzzard sand were investigated in the laboratory with a new micro-mechanical apparatus capable of imposing and measuring loads and deflections in both the normal and the tangential directions at the contacts of particles of sand to gravel size. The effects of the sliding velocity, the confining force and pre-shearing on the inter-particle coefficient of friction as well as the differences between particles tested in dry and saturated states are presented and discussed. Leighton Buzzard sand quartz particles were chosen in this study because of their relatively regular shape and consistent surface roughness.

2. Laboratory equipment

The new micromechanical apparatus and the repeatability of the experimental data on reference particles (chrome steel balls) have been presented by Senetakis and Coop (2013). In that study, Senetakis and Coop showed that the use of load cells and displacement transducers of high resolution as well as the use of high quality amplifiers, signal conditioning and a data logging system allows for the performance of tests in the range of very small displacements of the order of less than one to hundreds of microns, while the effect of environmental and electrical noise on the experimental data is minimized. The stiffness of the apparatus in the direction of sliding is sufficiently high in order to prevent stick-slip, while the stiffness in the vertical direction approaches that of apparatuses commonly used for particle crushing tests (Senetakis and Coop, 2013).

The basic concept of the new apparatus is that one particle, of sand to gravel size, is imposed to slide on the surface of a second particle, stationary in the direction of sliding. A simple scheme of the experimental equipment is given in Fig. 1. The particles are glued with epoxy on brass mounts which are fixed in brass wells. The lower well is attached to a stainless steel sled, 6 mm in thickness and 60×60 mm in plan. The sled is connected to a linear micro-stepping motor which moves the

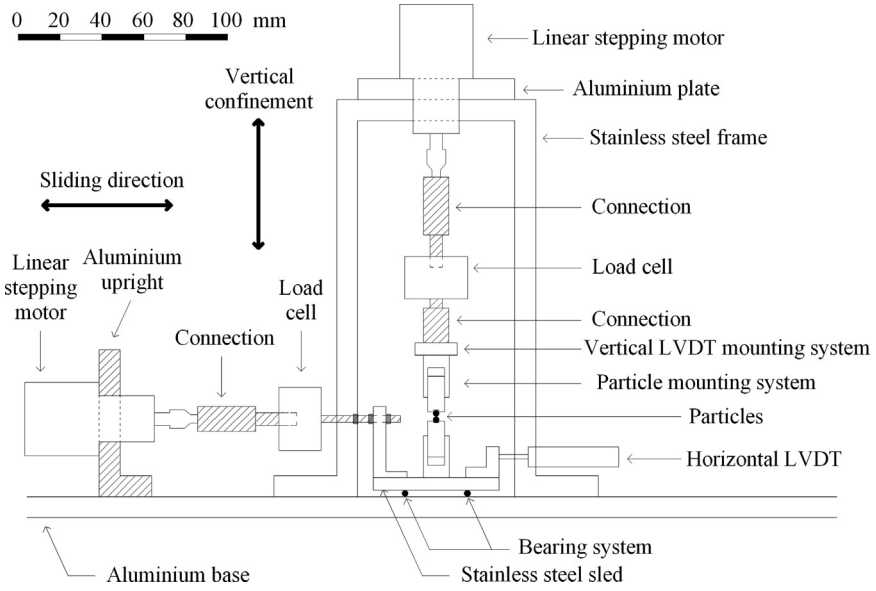

Fig. 1. General scheme of inter-particle loading apparatus (Senetakis and Coop, 2013).

lower particle with a target sliding velocity. This stepping motor is connected to a load cell that measures the horizontal force at the contact of the particles through a series of stiff mechanical parts. The upper well is connected to a linear micro-stepping motor that applies vertical confinement at the contacts of the particles, a load cell and a series of connecting parts. The horizontal system is held in place by a stiff aluminum upright, which is fixed on an aluminum base, while the vertical system is attached to a thick aluminum plate, which is fixed on a stiff stainless steel frame. A bearing system of three steel balls is used beneath the sled, while a thin stainless steel plate is located between the sled and the aluminum base to minimize the friction of the bearing system.

Linearly variable differential transformers (LVDTs), of a high resolution of about ± 0.1 μm, are used to record the horizontal displacement of the lower particle in the direction of shearing and the response of the upper particle in the vertical direction. A close-up view during a shearing test on chrome steel balls is shown in Fig. 2. As shown in this figure, the vertical LVDT is attached on the sled through a linear bearing composed of a block and a rail.

In order to maintain the sliding of the lower particle in a constant track, the sled is constrained to move laterally through the system shown in Fig. 3. In the out-of-plane direction, the sled is connected to an external upright through a similar linear bearing as the one used to attach the vertical LVDT to the sled. The friction produced by the linear bearings and the bearing system beneath the sled can be calibrated easily using simple laboratory procedures (Senetakis and Coop, 2013).

In recent studies using DEM (e.g., Barreto, 2009), it was revealed that the contact forces in granular assemblies and for isotropic pressures in the range of 100–400 kPa are of very small magnitude, with maximum values typically between 1 N and 4 N. Therefore, it was of key importance to use load cells of high stiffness that will allow the performance of shearing

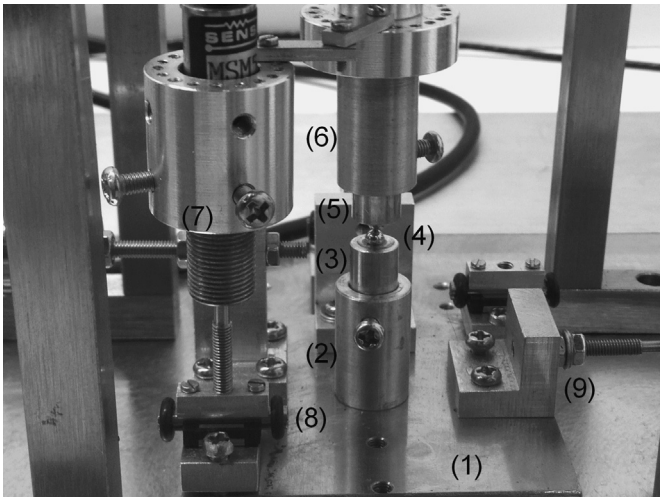

Fig. 2. Close-up view of apparatus: (1) stainless steel sled; (2) lower well; (3) lower mount; (4) particles; (5) upper mount; (6) upper well; (7) vertical LVDT; (8) linear bearing; and (9) armature of the horizontal LVDT.

tests without stick–slip, but also of high resolution (0.02 N in this study) in order to provide high quality data in the range of small forces, typically between 1 and 20 N.

In order to perform tests on particles immersed in liquid, typically distilled water, a small cell with an aluminum frame covered with plexiglas was constructed. A general view of the apparatus during the performance of a test on particles immersed in distilled water is given in Fig. 4. As shown in this figure, two digital micro-cameras are used in order to check the alignment of the particles and to record the tests. Two different stainless steel frames with slightly different levels of stiffness, denoted as “Frame 1” and “Frame 2”, were used. Senetakis and Coop (2013) showed that, when Frame 1 or Frame 2 is used, the differences in the results of the inter-particle shearing tests on the reference particles are negligible.

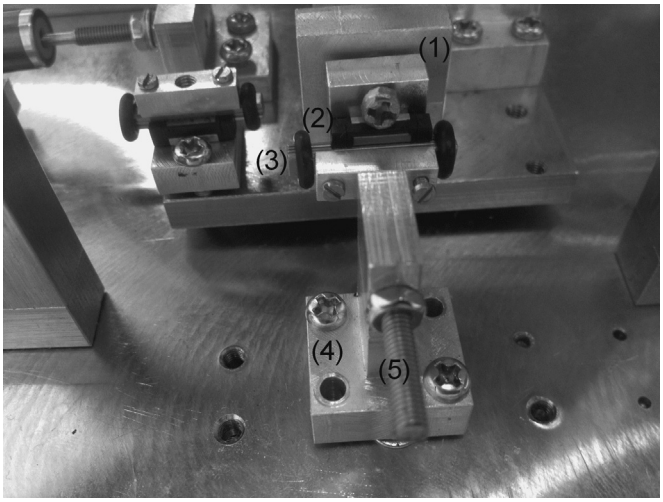

Fig. 3. Out-of-plane confining system of sled: (1) aluminum upright; (2) block of the linear bearing; (3) rail of the linear bearing; (4) external upright; and (5) M3 screw.

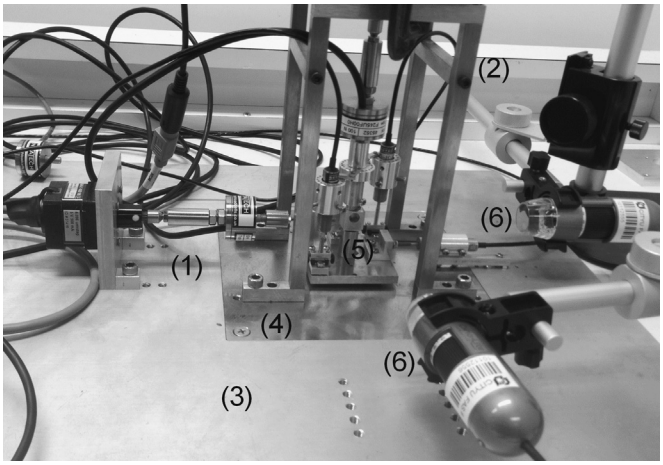

Fig. 4. Experiment on particles immersed in distilled water: (1) the horizontal loading system in the direction of sliding; (2) stainless steel frame where the vertical loading system is attached; (3) aluminum base; (4) stainless steel thin layer beneath bearing system of sled; (5) cell; and (6) digital micro-cameras (Senetakis and Coop, 2013).

3. Particle description, preparation and alignment

3.1. Particle description

Quartz particles of Leighton Buzzard sand, fractions 1.18–2.36 and 2.36–5.00 mm, were tested in this study. The surface roughness and the shape of the particles were evaluated using white light interferometry and a Sympatec QicPic lazer scanner, respectively. A flattened three-dimensional view of the surface of a typical particle is shown in Fig. 5, while a silhouette and shape parameters of a particle are given in Fig. 6. These shape parameters are described in detail by Cavarretta et al. (2010).

The surface roughness of the particles was calculated by the root mean square deviation of the heights of the surface, S_q, from Eq. (1).

$$S_q = \sqrt{\frac{1}{m \times n}\sum_{ij} z_{ij}^2} \quad (1)$$

where m and n are the number of points in the x-y plane and z is the deviation at each point from the mean height value (e.g., Cavarretta et al., 2010; Altuhafi and Coop, 2011).

An area of 20×20 μm was selected to achieve a sufficient resolution and to avoid undetected points on the particle surface. The roughness value was determined by flattening the surface shape in order to avoid the possible influence of the curvature of the particle shape on the value calculated. Through a series of interferometer tests on about 50 particles, from the same sample from which the particles for the shearing tests were selected, it was demonstrated that the particles show a consistent surface roughness with an average value of 0.38 μm and a standard deviation of ± 0.19 μm.

3.2. Particle selection and preparation

The particles used in this study were carefully selected in order that they would have relatively spherical shapes. The selection was carried out in two steps; a number of particles were selected from a particular fraction (1.18–2.36 or 2.36–5.00 mm) after visual observation, and thereafter, the most spherical particles among them were selected by observation through an optical microscope. The selected particles were washed with distilled water and oven-dried at 105 °C. Then, the particles to be tested were glued onto the brass mounts. Before the shearing tests, the surfaces of the particles were carefully cleaned using butanone. In the series of tests on particles in a dry state, some samples were oven-dried after being glued on the mounts and before the performance of the shearing tests in order to remove the humidity absorbed at the surfaces of the particles, while other samples were tested without being oven-dried. However, these two different stages of sample preparation did not produce any significant variation in the experimental data.

3.3. Particle alignment

The alignment of the particles at the initial position prior to shearing was checked through digital micro-cameras (shown in Fig. 4) from two different views, one in the direction of shearing and one in the out-of-plane direction. A typical example of the alignment of the particles at their initial position in the direction of shearing is given in Fig. 7. The maintenance of the particles close to their apexes in the out-of-plane direction was of crucial importance to obtaining reliable results (Cavarretta et al., 2011); and thus, this alignment was also checked during the shearing tests.

4. Calculations

The tangential force, F_T, the normal force, F_N, and therefore, the inter-particle coefficient of friction, μ, are calculated from

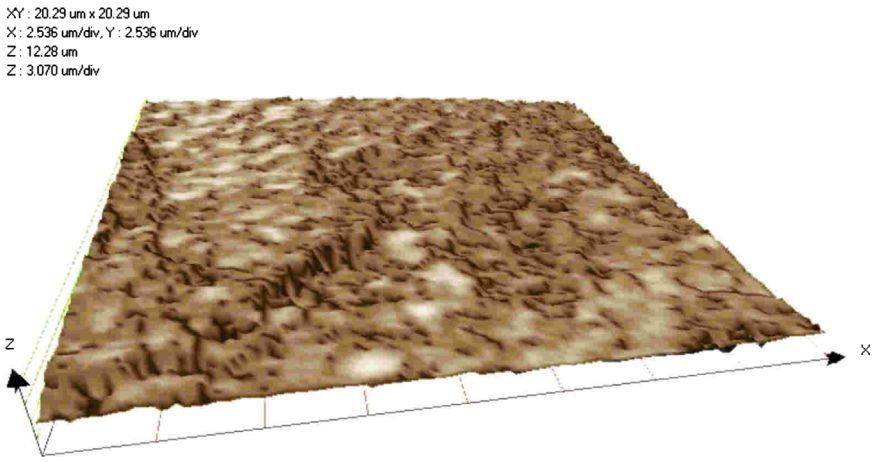

Fig. 5. Typical flattened three-dimensional view of surface of Leighton Buzzard sand quartz particle through white light interferometry.

EQPC	1143.918μm
FERET_MAX	1380.386μm
FERET_MIN	1065.372μm
Sphericity	0.901
Aspect ratio	0.772
Convexity	0.974
Elongation	0.507
Image number	94

Fig. 6. Binary image and shape parameters of typical Leighton Buzzard sand quartz particle.

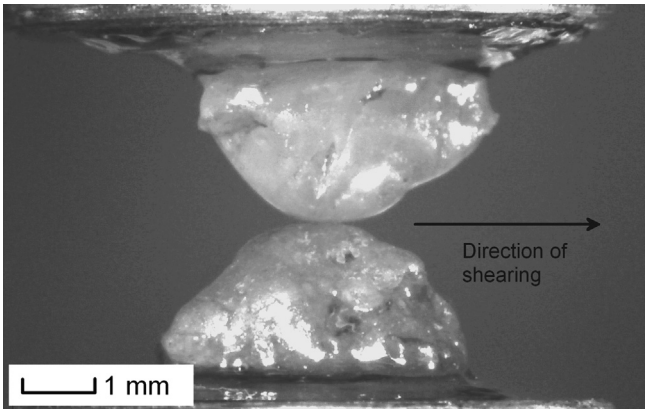

Fig. 7. Typical alignment of soil particles before performance of inter-particle shearing test.

the horizontal force, F_h, the vertical force, F_v, and the relative positions of the particles during shearing, which gives the angle, α, between the tangential force and the horizontal (Cavarretta et al., 2010, 2011). This angle is calculated by differentiating the vertical displacement with respect to the horizontal. Fig. 8 illustrates the forces at the contact of ideal spherical particles, the angle α and the response of the upper-stationary particle which is a function of the relative positions of the two particles.

In the majority of the inter-particle shearing tests in this study, the initial positions of the particles at the start of shearing corresponded to cases (b) or (c) in Fig. 8; and thus, the response of the upper particle in the vertical direction followed the track B→C→D or C→D. From simple

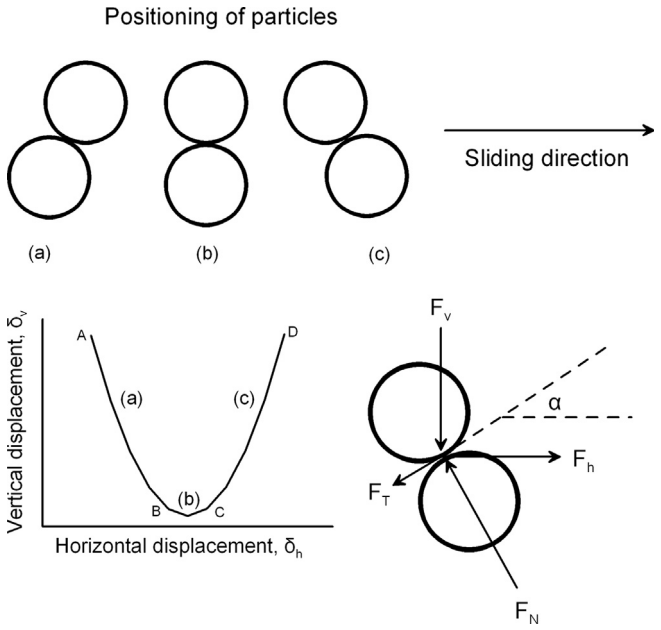

Fig. 8. Forces developed at contacts of particles during shearing test where upper particle is stationary in direction of sliding (Senetakis and Coop, 2013).

geometry, the inter-particle coefficient of friction, μ, and the forces F_N and F_T, can be determined through Eqs. (2)–(4).

$$\mu = \frac{F_h \times \cos\alpha - F_v \times \sin\alpha}{F_h \times \sin\alpha + F_v \times \cos\alpha} \tag{2}$$

$$F_N = \frac{F_v \times \sin\alpha}{\cos\alpha - \mu \times \sin\alpha} \tag{3}$$

$$F_T = \mu \times N \tag{4}$$

5. Testing program

A series of 26 inter-particle shearing tests of a displacement-controlled type was carried out in this study. Seventeen tests were performed on particles in a dry state at room temperature of 23.5 °C ± 1 °C, a relative humidity of 93–97% and sliding

velocities between 200 and 1000 μm/h. Nine tests were performed on particles immersed in distilled water with a range of sliding velocities between 600 and 900 μm/h. The vertical confining force was held constant during the shearing tests and varied between 1 and 16 N. The time interval of the data logging the output from the transducers ranged from 6 to 12 s. The total shearing track ranged from 80 to 250 μm in most tests.

The shearing tests of a displacement-controlled type focused on the coefficient of dynamic friction, μ_{dyn}, i.e., the frictional response during constant shearing, with limited information for the response before the onset of a steady-state sliding. For this reason, a series of 38 shearing tests of a force-controlled type, with a time interval for the data logging of about 1 s, was also carried out. These experiments provided more detailed information for the tangential force–displacement response before the onset of steady-state sliding and the coefficient of static friction μ_{st}.

6. Experimental results and discussion

6.1. Coefficient of dynamic friction through tests of a displacement-controlled type

The resultant coefficient of dynamic friction, μ_{dyn}, calculated along the shearing track for representative tests of a displacement-controlled type is given in Fig. 9 for particles in a dry state and in Fig. 10 for particles immersed in distilled water. Depending on the initial positions of the particles at the start of shearing and the morphology of the particles, the inter-particle coefficient of friction may initially increase or decrease slightly. In the tests presented in Figs. 9 and 10, the mean μ_{dyn} value as well as the standard deviation of the parameter along the shearing track, μ_{dyn}, are also quoted. The inter-particle coefficient of friction is fairly similar for the particles tested in the dry and saturated states.

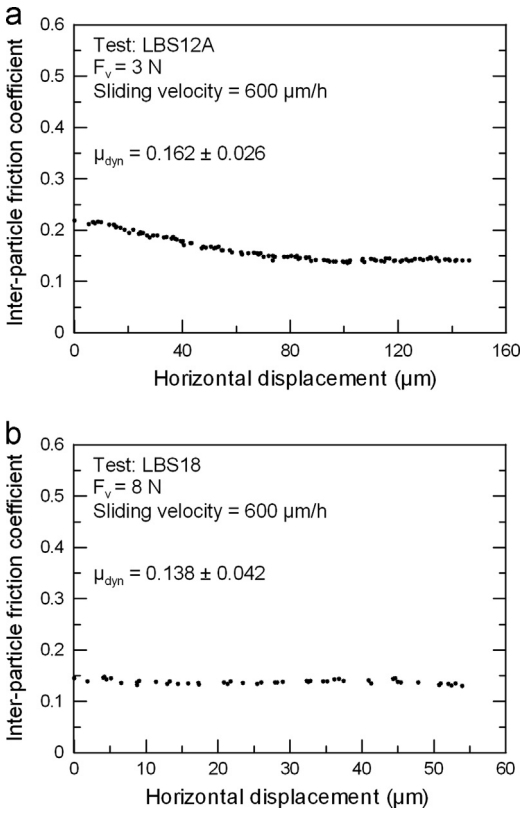

Fig. 9. Dynamic coefficient of friction along the shearing track of particles in dry state – representative results from tests of displacement-controlled type (average value ± standard deviation is quoted).

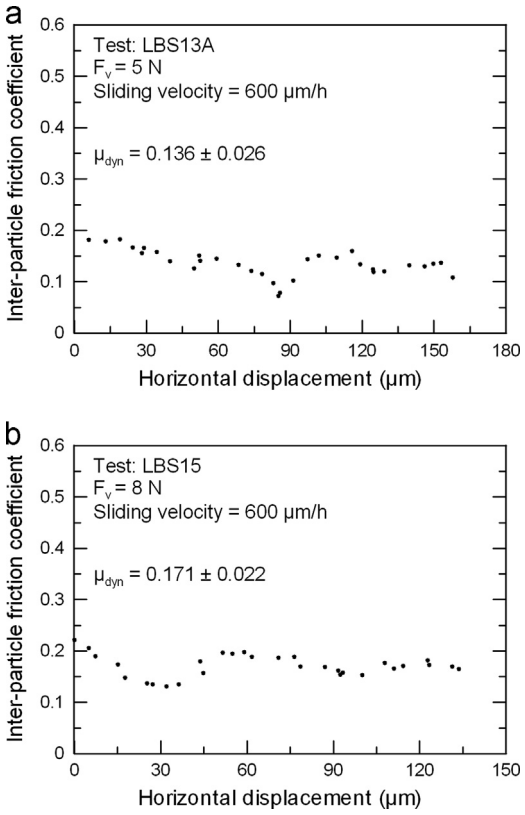

Fig. 10. Dynamic coefficient of friction along the shearing track of particles immersed in water – representative results from tests of displacement-controlled type (average value ± standard deviation is quoted).

In Table 1, the 26 inter-particle shearing tests of a displacement-controlled type are summarized. In this table, the coefficient of dynamic friction, μ_{dyn}, and the inter-particle friction angle, φ_{dyn}, expressed as mean values along the shearing track, are also quoted. For the particles tested in a dry state, the inter-particle coefficient of friction varies in a narrow range between 0.093 and 0.231. For the particles tested in a saturated state, the values of the inter-particle coefficient of friction are fairly similar to the tests in a dry state, ranging between 0.114 and 0.193. From Table 1, it is also demonstrated that for the range in vertical confining forces, F_v, between 0.9 and 16 N, and sliding velocities, between 200 and 1000 μm/h, the effects of F_v and the sliding velocity on the frictional characteristics at the particle contacts seem to be negligible. These data show reasonable repeatability of the resultant inter-particle coefficient of friction during constant shearing, which is possibly attributed to the consistent surface roughness of the particles included in this study.

Table 1
Summary of inter-particle shearing tests of displacement-controlled type on Leighton Buzzard sand quartz particles.

Code of test	Particle size (mm)	State	Sliding velocity (μm/h)	F_v (N)	μ_{dyn} [c]	φ_{dyn} [c] (deg)	Frame
LBS01A	2.36–5.00	Dry[a]	200	2	0.128	7.3	1
LBS01B	2.36–5.00	Dry	200	2	0.106	6.1	1
LBS02	2.36–5.00	Dry	200	2	0.150	8.5	1
LBS03	2.36–5.00	Dry	200	2	0.156	8.9	1
LBS04	2.36–5.00	Dry	300	5	0.145	8.3	1
LBS05A	2.36–5.00	Dry	300	5	0.179	10.2	1
LBS05B	2.36–5.00	Dry	300	5	0.170	9.7	1
LBS06	2.36–5.00	Dry	600	8	0.123	7.0	2
LBS07	2.36–5.00	Dry	600	16	0.231	13.0	2
LBS08	1.18–2.36	Dry	600	3	0.115	6.6	2
LBS09	2.36–5.00	Dry	600	0.9	0.216	12.2	2
LBS10	1.18–2.36	Dry	1000	10	0.195	11.0	2
LBS11	2.36–5.00	Dry	600	12	0.171	9.7	1
LBS12A	2.36–5.00	Dry	600	3	0.162	9.2	1
LBS12B	2.36–5.00	Dry	600	3	0.150	8.5	1
LBS13A	1.18–2.36	Saturated[b]	600	5	0.136	7.8	1
LBS13B	1.18–2.36	Saturated	600	5	0.114	6.5	1
LBS14	2.36–5.00	Saturated	600	8	0.193	10.9	1
LBS15	2.36–5.00	Saturated	600	8	0.171	9.7	1
LBS16	2.36–5.00	Saturated	600	8	0.191	10.8	1
LBS17	2.36–5.00	Saturated	900	5	0.135	7.7	1
LBS18	2.36–5.00	Dry	600	8	0.138	7.9	2
LBS19	1.18–2.36	Dry	600	0.9	0.093	5.3	1
LBS20	2.36–5.00	Saturated	900	5	0.154	8.8	1
LBS21	2.36–5.00	Saturated	900	5	0.128	7.3	1
LBS22	2.36–5.00	Saturated	900	5	0.163	9.3	1

[a]Dry state: particles tested at a relative humidity of about 93–97%.
[b]Saturated state: particles immerged in distilled water.
[c]Mean values along the shearing track.

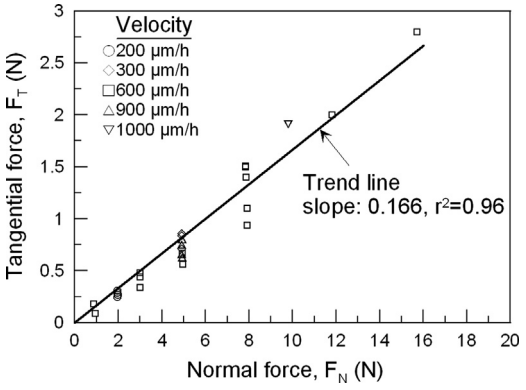

Fig. 11. Tangential force F_T against normal force F_N for 26 shearing tests of displacement-controlled type on Leighton Buzzard sand quartz particles at variable sliding velocities (F_N and F_T correspond to mean values along the shearing track, slope of trend line corresponds to dynamic coefficient of friction).

In a limited number of samples, the effect of pre-shearing on the coefficient of dynamic friction was investigated. For example, after the performance of test LBS01A, the vertical confinement was released, the particles were aligned at the same initial positions and a second shearing test, named LBS01B, was carried out at the same sliding velocity and vertical force following the same shearing track. Similar repeating tests were performed in the series LBS05A–LBS05B, LBS12A–LBS12B and LBS13A–LBS13B. These tests demonstrated that after the first shearing, there is a small reduction in the inter-particle coefficient of friction (for example, from 0.128 to 0.106 in tests LBS01A-LBS01B and from 0.179 to 0.170 in tests LBS05A-LBS05B). De la Hire (summarized by Mate, 2008) suggested that one of the main mechanisms that contributes to the development of friction between rough surfaces is the plastic deformation of the asperities. It is possible that this small reduction in the inter-particle friction angle after the first shearing can be partially attributed to some damage of the asperities. In this study, the surface roughness of the particles was investigated only before the shearing tests; further research is needed to quantify the effect of shearing and the number of shearing cycles on particle roughness. Unfortunately, this is technically very difficult as it requires very precise imaging of the exact location of the contact track between the particles. Senetakis et al. (2013b) described a technique that may be used to identify the shearing track, using the interferometry principle when a particle–particle type of contact is considered, and the possible damage to the asperities. They showed that for quartz particles, a decrease in the static coefficient of friction is observed after the first shearing and that this was primarily attributed to the removal of asperities.

The tangential force, F_T, is plotted against the normal force, F_N, for all tests of a displacement-controlled type in Fig. 11. The F_T and F_N values of this figure correspond to the mean

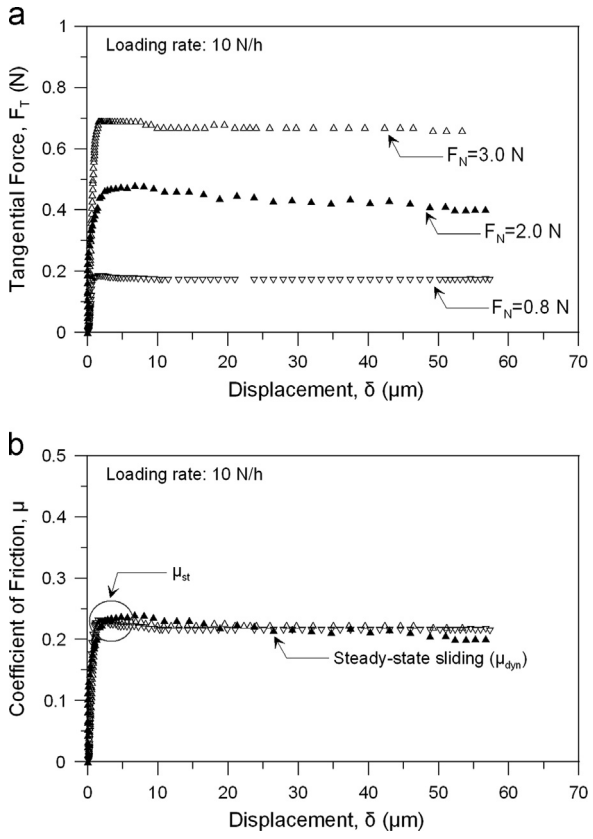

Fig. 12. Tangential force–displacement and coefficient of friction–displacement response at contacts of dry particles through tests of force-controlled type and effect of normal load.

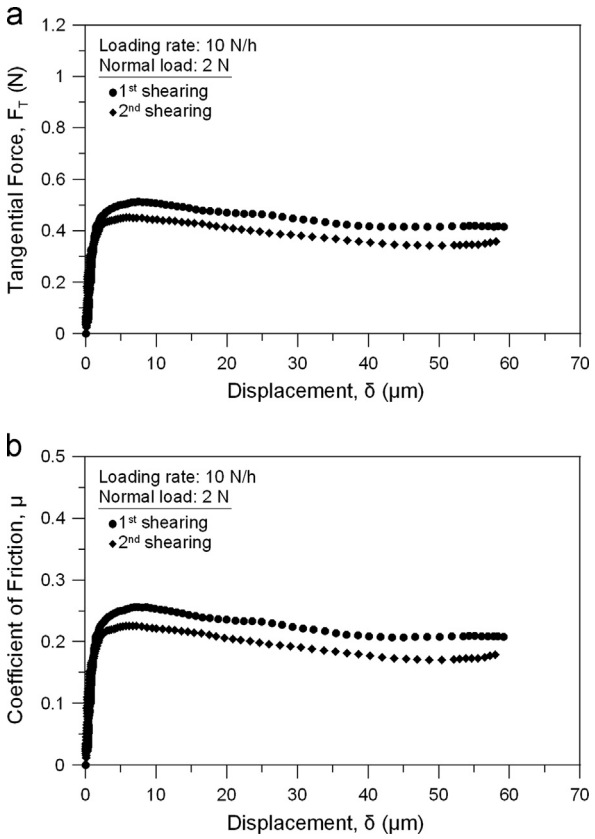

Fig. 13. Tangential force–displacement and coefficient of friction–displacement response at contacts of dry particles through tests of force-controlled type and effect of repeating shearing.

values along the shearing track. These results show that, within the scatter of the data, there is a linear envelope which demonstrates that the coefficient of dynamic friction is independent of the force level. The average coefficient of dynamic friction that corresponds to the slope of the F_T–F_N fitting curve is equal to 0.166. It is also noted that the linear envelope passes through the origin; this is an indication that the corrections to the data for the apparatus friction are accurate.

6.2. *Static coefficient of friction through tests of a force-controlled type*

Typical tangential force–displacement diagrams from the tests of a force-controlled type are given in Fig. 12(a). These data correspond to a pair of particles subjected to increasing normal loads from 0.8 to 3.0 N. Initially, the tangential force increased abruptly. The onset of a steady state sliding was observed at displacements between about 0.5 and 3.0 μm in most experiments. The corresponding mobilized coefficients of friction are plotted against the displacement in Fig. 12(b). These tests did not show any significant effect of the normal load on the frictional characteristics at the contacts of the particles. For these experiments, the coefficient of static friction ranged from about 0.23 to 0.24 with very similar values for the coefficient of dynamic friction.

The effect of repeating shearing on the static and dynamic coefficients of friction from the tests of a force-controlled type is plotted in Fig. 13. These tests corresponded to a normal load of 2.0 N. As for the displacement-controlled tests, it was revealed that a small reduction in the coefficient of friction for both the initial response and beyond a steady state of sliding was reached, as is shown in the figure. In these tests, a very slight decrease in the coefficient of friction was also observed beyond the steady state.

Fig. 14 summarizes the results of the shearing tests of a force-controlled type in terms of the tangential force at the onset of a steady-state sliding plotted against the normal force. The envelope shown in this figure corresponds to the coefficient of static friction. As for the tests of a displacement-controlled type, a linear envelope was observed which demonstrates that the static friction is almost independent of the normal load. In the same figure, the trend line from the displacement-controlled tests presented in Fig. 11 is also plotted for comparison. These data show that the average coefficient of dynamic friction was slightly lower than the coefficient of static friction, but within the scatter of the data the differences may not be significant.

7. Conclusions

The results of a series of inter-particle shearing tests on quartz particles of Leighton Buzzard sand have been presented

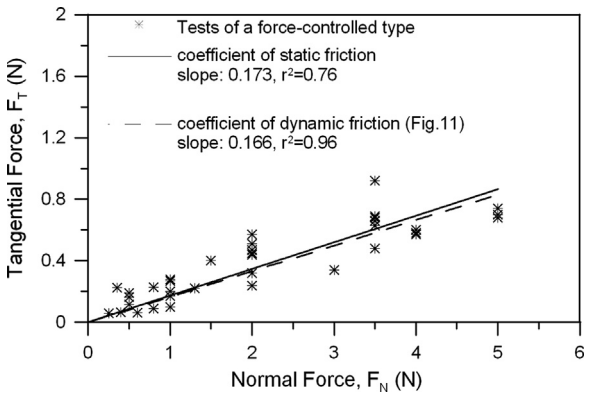

Fig. 14. Normal force F_N against tangential force F_T for 38 shearing tests of force-controlled type on Leighton Buzzard sand quartz particles (F_N and F_T correspond to the onset of steady state sliding).

in this paper. A new apparatus capable of imposing and measuring forces and deflections in the normal and the tangential directions, at the contacts of soil particles of sand to gravel size, was developed for this purpose, the main features of which were described briefly. The shape and surface roughness of the particles were evaluated using advanced laboratory techniques. White light interferometry images showed that the roughness of the particles is consistent with an average value of 0.38 μm and a standard deviation of ± 0.19 μm.

The tests of a displacement-controlled type showed reasonable repeatability of the resultant coefficient of dynamic friction μ_{dyn}, with values between 0.093 and 0.231 for particles tested in a dry state at room temperature and at a relative humidity of 23.5 °C ± 1 °C and 93% to 97%, respectively. Tests on particles immersed in distilled water showed very similar μ_{dyn} values to those in a dry state. The effect of the sliding velocity, ranging from 200 to 1000 μm/h, and the vertical confining force, ranging from 0.9 to 16 N, was very small on the resultant inter-particle coefficient of friction. Repeating inter-particle shearing tests showed a small reduction in the friction angle, which might be attributed to some damage at the asperities during the first shearing.

The tests of a force-controlled type provided information on the response at the contacts of the soil particles before a steady-state was reached. These tests showed that the coefficients of static and dynamic friction, μ_{st} and μ_{dyn}, respectively, were very similar. Steady state sliding was observed at displacements between about 0.5 and 3.0 μm in most experiments.

Acknowledgments

The authors would like to thank the anonymous reviewers for their constructive comments and their detailed suggestions which helped us to improve the quality of the paper. The technicians from City University of Hong Kong, Mr. L.C. Mac and Mr. C.K. Lai, and the Senior Technical Officer, Mr. K.H. Chu, are acknowledged for their technical support during the development of the new custom-built apparatus. Dr. Beatrice Baudet, from the University of Hong Kong, is also acknowledged for her invaluable help with the interferometer tests. The work described in this paper was fully supported by a grant from City University of Hong Kong (Project no. 7002667).

References

Altuhafi, F.N., Coop, M.R., 2011. Changes to particle characteristics associated with the compression of sands. Geotechnique 61 (6), 459–471.

Barreto, D., 2009. Numerical and Experimental Investigation into the Behaviour of Granular Materials under Generalised Stress States (Ph.D. thesis). University of London, Department of Civil Engineering, Imperial College of Science, Technology and Medicine.

Barreto, D., O' Sullivan, C., 2012. The influence of inter-particle friction and the intermediate stress ratio on soil response under generalised stress conditions. Granular Matter 14, 505–521.

Baumberger, T., Berthoud, P., Caroli, C., 1999. Physical analysis of the state- and rate-dependent friction low. II. Dynamic friction. Physical Review B 60 (6), 3928–3939.

Baumberger, T., Caroli, C., 2006. Solid friction from stick-slip down to pinning and aging. Advances in Physics 55 (3–4), 279–348.

Berthoud, P., Baumberger, T., G'Sell, C., Hiver, J.-M., 1999. Physical analysis of the state- and rate-dependent friction low. Static friction. Physical Review B 59 (22), 14313–14327.

Burwell, J.T., Rabinowicz, E., 1953. The nature of the coefficient of friction. Journal of Applied Physics 24 (2), 136–139.

Cavarretta, I., Coop, M.R., O' Sullivan, C., 2010. The influence of particle characteristics on the behavior of coarse grained soils. Geotechnique 60 (6), 413–423.

Cavarretta, I., Rocchi, I., Coop, M.R., 2011. A new interparticle friction apparatus for granular materials. Canadian Geotechnical Journal 48 (12), 1829–1840.

Cole, D.M., Peters, J.F., 2007. A physically based approach to granular media mechanics: grain-scale experiments, initial results and implications to numerical modeling. Granular Matter 9, 309–321.

Cole, D.M., Peters, J.F., 2008. Grain-scale mechanics of geologic materials and lunar simulants under normal loading. Granular Matter 10, 171–185.

Cole, D.M., Mathisen, L.U., Hopkinks, M.A., Knapp, B.R., 2010. Normal and sliding contact experiments on gneiss. Granular Matter 12, 69–86.

Consoli, N.C., Heineck, K.S., Coop, M.R., Viana da Fonseca, A., Ferreira, C., 2007. Coal bottom ash as a geomaterial: influence of particle morphology on the behaviour of granular materials. Soils and Foundations 47 (20), 361–374.

Cundall, P.A., Strack, O.D.L., 1979. A discrete numerical model for granular assemblies. Geotechnique 29, 49–65.

Fonseca, J., O'Sullivan, C., Coop, M.R., Lee, P.D., 2012. Non-invasive characterization of particle morphology of natural sands. 52 (4), 712–722.

Horn, H.M., Deere, D.U., 1962. Frictional characteristics of minerals. Geotechnique 12 (4), 319–335.

Jo, S.-A., Kim, E.-K., Cho, G.-C., Lee, S.-W., 2011. Particle shape and crushing effects on direct shear behavior using DEM. Soils and Foundations 51 (4), 701–712.

Krick, B.A., Vail, J.R., Persson, B.N.J., Sawyer, W.G., 2012. Optical in situ micro tribometer for analysis of real contact area for contact mechanics, adhesion, and sliding experiments. Tribology Letters 45, 185–194.

McDowell, G.R., Bolton, M.D., 1998. On the micromechanics of crushable aggregates. Geotechnique 48 (5), 667–679.

McDowell, G.R., Amon, A., 2000. The application of Weibull statistics to the fracture of soil particles. Soils and Foundations 40 (5), 133–141.

McDowell, G.R., 2002. On the yielding and plastic compression of sand. Soils and Foundations 42 (1), 139–145.

Mate, M., 2008. Tribology on the Small Scale—a Bottom Up Approach to Friction, Lubrication, and Wear. Oxford University Press, Oxford, UK.

Nakata, Y., Hyde, A.F., Hyodo, M., Murata, H., 1999. A probabilistic approach to sand particle crushing in the triaxial test. Geotechnique 49 (5), 567–583.

Procter, D.C., Barton, R.R., 1974. Measurements of the angle of interparticle friction. Geotechnique 24 (4), 581–604.

Sazzad, Md.M, Suzuki, K., 2011. Effect of interparticle friction on the cyclic behavior of granular materials using 2D DEM. Journal of Geotechnical and Geoenvironmental Engineering 137 (5), 545–549.

Senetakis, K., Coop, M.R., 2013. The development of a new micro-mechanical inter-particle loading apparatus. Geotechnical Testing Journal (submitted for publication).

Senetakis, K., Anastasiadis, A., Pitilakis, K., 2012. The small-strain shear modulus and damping ratio of quartz and volcanic sands. Geotechnical Testing Journal 35 (6)http://dx.doi.org/,10.1520/GTJ20120073.

Senetakis, K., Anastasiadis, A., Pitilakis, K., Coop, M.R., 2013a. The Dynamics of a pumice granular soil in dry state under isotropic resonant column testing. Soil Dynamics and Earthquake Engineering 45, 70–79.

Senetakis, K., Coop, M.R, Todisco, M.C., 2013b. Tangential load–deflection behaviour at the contacts of soil particles. Geotechnique Letters 3 (2), 59–66. http://dx.doi.org/,10.1680/geolett.13.00019.

Soga, K., O'Sullivan, C., 2010. Modeling of geomaterials behavior. Soils and Foundations 50 (6), 861–875.

Skinner, A.E., 1969. A note on the influence of interparticle friction on shearing strength of a random assembly of spherical particles. Geotechnique 19, 150–157.

Thornton, C., 2000. Numerical simulations of deviatoric shear deformation of granular media. Geotechnique 50 (1), 43–53.

Wang, J., Yan, H.B., 2012. DEM analysis of energy dissipation in crushable soils. Soils and Foundations 52 (4), 644–657 (online first).

Watanabe, Y., Lenoir, N., Otani, J., Nakai, T., 2012. Displacement in sand under triaxial compression by tracking soil particles on X-ray CT data. Soils and Foundations 52 (2), 313–320.

Yimsiri, S., Soga, K., 2000. Micromechanics-based stress–strain behaviour of soils at small strains. Géotechnique 50 (5), 559–571.